



Analysis and test results of a brushless doubly fed induction machine with rotary transformer

Fredemar Runcos
WEG
BRAZIL
fredemar@weg.net

Mauricio Ruviaro
WEG
BRAZIL
maurior@weg.net

Iduan Machado Borges
WEG
BRAZIL
iduanb@weg.net

Nelson Sadowski
UFSC
BRAZIL
nelson@grucad.ufsc.br

Abstract - This paper analyses a 90kW brushless doubly fed three-phase induction machine in which wound rotor circuit is connected to a rotary transformer. It presents the advantages of substituting brushes and slip-rings by rotary transformer. In addition, it shows rotary transformer design and presents the doubly fed induction machine operation. The steady state model considers electrical circuit techniques to provide information about current, power factor and efficiency on load. Equivalent circuit parameters are obtained through laboratory tests under a prototype. Comparisons between simulation and measurement results attest the good performance of the adopted model.

INDEX TERMS: AC MOTORS, BRUSHLESS MACHINES, CIRCUIT ANALYSIS, CIRCUIT SIMULATION, EQUIVALENT CIRCUITS, INDUCTION MOTORS, PROTOTYPE, ROTATING MACHINES, ROTARY TRANSFORMER, TEST FACILITIES;

NOMENCLATURE

Induction machine parameters:

V_{lm1} : stator winding line voltage, [V]
 V_{lm2} : rotor winding line voltage, [V]
 V_{m1} : stator winding single-phase voltage, [V]
 V_{m2} : rotor winding single-phase voltage, [V]
 I_{m1} : stator winding current, [A]
 I_{mm} : magnetizing current, [A]
 I'_{m2} : rotor winding current, [A]
 P_{m1} : power absorbed or delivered to the grid, [kW]
 $P_{air-gap}$: power on the air-gap, [kW]
 P_{shaft} : mechanical power on shaft, [kW]
 f_{m1} : stator winding electric frequency, [Hz]
 f_{m2} : rotor winding electric frequency, [Hz]
 f_{mec} : mechanical frequency, [Hz]
 f_{syn} : synchronous mechanical frequency, [Hz]
 R_{m1} : stator winding resistance, [Ω]
 X_{m1} : stator winding leakage reactance, [Ω]
 R_{mfe1} : stator iron resistance, [Ω]
 X_{mm} : magnetizing reactance, [Ω]
 R_{mfe2} : rotor iron resistance, [Ω]
 R'_{m2} : rotor winding resistance, [Ω]
 X'_{m2} : rotor winding leakage reactance, [Ω]
 p_m : number of poles pairs
 s : slip of induction machine

Rotary transformer parameters:

V_{t1} : stator winding single-phase voltage, [V]
 V_{t2} : rotor winding single-phase voltage, [V]
 I'_{t1} : stator winding current, [A]
 I'_{tm} : magnetizing current, [A]
 I'_{t2} : rotor winding current, [A]
 S_t : apparent power of rotary transformer, [kVA]
 N_{t1} : number of turns at stator winding
 N_{t2} : number of turns at rotor winding

R'_{t1} : stator winding resistance, [Ω]
 X'_{t1} : stator winding leakage reactance, [Ω]
 R'_{tfe1} : stator iron resistance, [Ω]
 X'_{tm} : magnetizing reactance, [Ω]
 R'_{tfe2} : rotor iron resistance, [Ω]
 R'_{t2} : rotor winding resistance, [Ω]
 X'_{t2} : rotor winding leakage reactance, [Ω]
 R'_{ext} : external resistance, [Ω]

1. INTRODUCTION

Three-phase induction machine is a popular motor for industrial application and a largely used generator in wind energy farms. In this context doubly fed induction machines demands special attention regarding its features on torque and speed controllability [1] - [17]. Speed and torque can be controlled by rheostats or frequency converter via rotor winding. Connected to induction machine rotor circuit, the converter processes an amount of power proportional to rotor speed. This arrangement reduces converter power to a fraction of the total mechanical power, saving costs [1] - [4], [15]. The benefits of doubly fed induction machines use are undeniable; nevertheless, to take advantages of them it is necessary to provide electrical connection between rotor winding and statics rheostat or frequency converter [1] - [17]. Nowadays, the most common way to access rotor winding is by brushes and slip-rings. However, the mechanical contact between moving slip-rings and static brushes wears these components and involves maintenance of them. Powder generated by brushes wearing can be also prejudicial for



motor insulation. Additionally, any fault on electrical contact can generate sparks, limiting machine installation only to non-explosive environments [1].

Development of brushless technologies is very interesting for reducing maintenance costs and expanding the use doubly fed machines to explosive atmospheres [1] – [12], [18].

Many studies consider the use of two induction machines connected in cascade for obtaining brushless devices. One possibility consists in mounting two individual machines (each one with its own rotor and stator) on the same shaft with electrical connection between their rotors windings [2]. Another one is represented by manufacturing a double winding stator and a special rotor cage able to join two different induction machines in one single frame [3] – [11].

The combination of two induction machines is effective at the view of eliminating brushes and slip-rings, but introduces superposition of two different torque behaviors. The result is a device with an anomalous torque vs. speed curve, in which synchronous speed is determined by the combination of each machine number of poles [2], [3].

Only the combination of the induction machine with a device lacking in any torque would allow no changes on synchronous speed and on torque vs. speed curve shape.

Since the seventies, it has been made several studies in order to substituting brushes and slip-rings by contactless energy transfer systems, as, for example, rotary transformers [18] – [26].

Initially, this device was developed concerning spacecrafts applications, where the lack of reliability and high rate of maintenance of brushes and slip-rings are totally undesirable [18].

In [20], Papastergiou and Macpherson propose rotary transformer as an alternative solution for contactless transfer of energy across the revolving frame of airborne electronic-scanning radar. In [28], Legranger et al. propose the replacement of gliding contacts of a wound rotor synchronous machine by an axial rotary transformer operating as contactless transmission power system.

Despite of some particularities, all of these usages for rotary transformer involve applications where the transformer is submitted to frequencies of hundreds of Hz [18] – [28].

In [1], nevertheless it is presented the use of rotary transformer electrically connected to an induction machine rotor circuit in a way practically not studied until nowadays.

Figure 1 presents the doubly fed three-phase induction machine with rotary transformer.

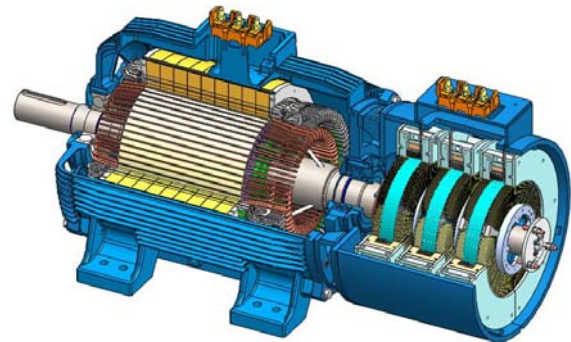


Figure 1 - Doubly fed three-phase induction machine with rotary transformer

Working with induction machine rotor frequency, the rotary transformer allows the access to rotor circuit without any mechanical contact. By using an appropriated drive, it is possible to control the induction machine to operate as a generator as well as a motor at almost any speed, except on synchronicity.

As well as conventional doubly fed induction machines, the solution presented in Figure 1 is very convenient for systems that must generate constant frequency voltage by the use of variable speed devices, like wind turbines [1] - [17].

To evaluate the proposed device capabilities, it is important to use a pertinent analytical model not only to aide in the machine design but also to have a better insight on its peculiar characteristics mainly concerning the rotary transformer [1]. This paper shows transformer main design aspects and doubly fed machine operation; it discusses about the steady state model that enables performance prediction of the doubly fed three-phase induction machine with rotary transformer. Results presented on this paper are based on laboratory tests under a 90kW prototype.



2. ROTARY TRANSFORMER DESIGN

Rotary transformer design [1], [18] - [26], different from conventional transformers, has the particularity of an air-gap to permit movement between primary (stator) and secondary (rotor) windings as can be observed in Figure 2.

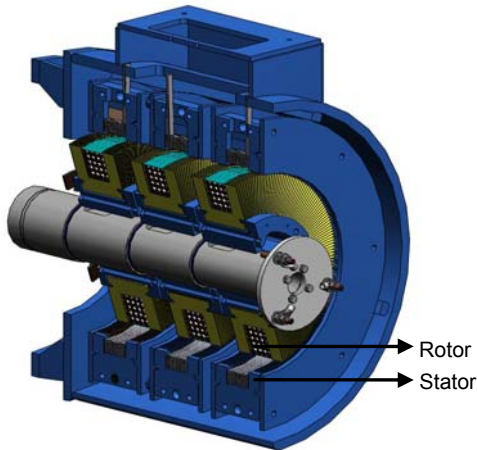


Figure 2 - Design of three-phase rotary transformer system

The three transformers are shell-form with primary and secondary windings totally involved by the core. The option for 3 single-phase units design has the objective to reduce flux unbalance on rotary transformer system. The presence of air-gap introduces reluctances that change the magnetic circuit in comparison to conventional transformers [1].

Core magnetic permeability is much higher than air-gap permeability. For a non-saturated core, air-gap reluctance is high and affects transformer magnetizing reactance. Like other devices for contactless energy transmission [5], rotary transformer has high leakage/magnetizing reactance ratio.

Figure 3 and table 1 present main dimensions of the designed single-phase rotary transformers.

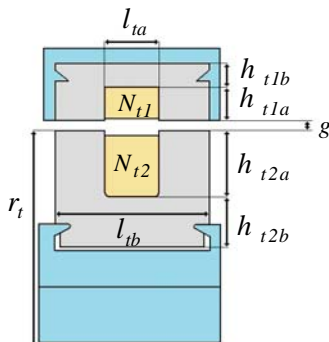


Figure 3 - Single-phase rotary transformer

Table 1 - Rotary transformer dimensions

h_{t1a}	h_{t1b}	h_{t2a}	h_{t2b}	N_{t1}
32mm	21mm	65mm	33mm	19
l_{ta}	l_{tb}	r_t	g	N_{t2}
52mm	110mm	192mm	1,5mm	19

In the developed prototype, rotary transformer core was made of laminated silicon steel. As can be observed in Figure 2, lamination direction is longitudinal to the shaft.

The permanent alignment of rotor and stator windings results in no slip between their magnetic fields. As consequence, rotary transformer produces no torque on shaft.

3. DOUBLY FED INDUCTION MACHINE OPERATION

The doubly fed induction machine with rotary transformer is the set of a three-phase induction machine with 2pm poles stator winding directly connected to the electrical grid and a three-phase rotary transformer whose stator winding can be short-circuited or connected to rheostat banks or to electrical grid through a vector-controlled frequency converter [1] - [3].

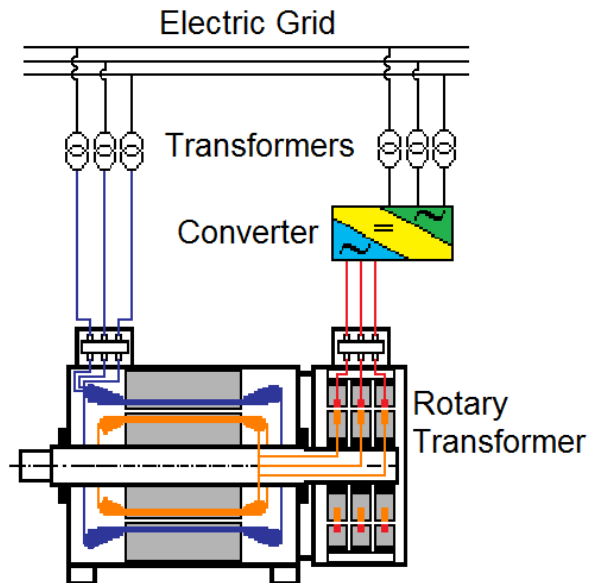


Figure 4 - Grid connection of the doubly fed three-phase induction machine with rotary transformer

Electrical connections for the use of converter are shown in Figure 4. This configuration allows controlling torque, speed, power factor and current of induction machine by the converter connected to the stator winding of rotary transformer. The frequency converter controls the machine acting on amplitude, frequency and phase of voltage applied in stator winding of rotary transformer [1] -



[3].
When the stator winding of rotary transformer is connected only to a resistive bank, it is possible to control torque, speed and current. However, power factor is not controllable [1].
In the built prototype, all electrical connections were in Y. Nevertheless, design for connection in D is perfectly possible.
Being a brushless system is the greatest advantage of the solution shown in Figures 1 and 4.
The rotary transformer permits to adjust its stator voltage (V_{t1}) only changing the relation of turns between the primary (N_{t1}) and secondary windings (N_{t2}):

$$V_{t1} = (N_{t1}/N_{t2}) \cdot V_{t2} \quad (1)$$

The only requirement is the same voltage for induction machine (V_{m2}) and rotary transformer rotor (V_{t2}):

$$V_{m2} = V_{t2} \quad (2)$$

The fundamental frequency of the air-gap induction wave generated by the induction machine stator winding induces a rotor winding current with electric frequency f_{m2} given by:

$$f_{m2} = f_{m1} - p_m f_{mec} \quad (3)$$

Rotor winding of the induction machine is electrically connected to rotor winding of the transformer; consequently their currents have the same electric frequency f_{m2} .
Despite mechanical movement between rotor and stator transformer, there is no slip between their magnetic flux. Currents on rotor and stator windings are also in frequency f_{m2} .
The synchronous mechanical frequency f_{syn} is:

$$f_{syn} = f_{m1} / p_m \quad (4)$$

The mechanical frequency of the shaft of the machine is:

$$f_{mec} = (f_{m1} - f_{m2}) / p_m \quad (5)$$

Equation (5) shows that it is possible to control the speed of induction machine by changing the frequency f_{m2} of the voltage on stator winding of rotary transformer [1] - [17].
When the converter is connected to stator winding of the transformer, as shown in Figure 4, frequency, amplitude and phase of the voltage can be imposed on transformer stator, allowing in this way a complete control of the doubly fed induction machine. This control is not possible only at synchronous speed, when electric frequency on

rotary transformer is null and it is impossible to transmit energy between its rotor and stator. This energy transference depends necessarily of alternating current (AC) presence.
Figure 5 shows the frequency on induction machine stator and induced frequencies on induction machine rotor and transformer windings. Induced electric frequencies are function of mechanical frequency or speed of machine shaft. The synchronous rotating frequency is represented by f_{syn} .

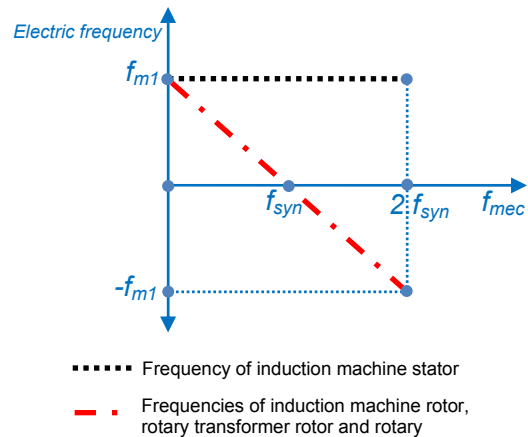


Figure 5 - Current frequency in induction machine and rotary transformer

4. STEADY-STATE MODEL

The steady-state behavior is obtained through machine equivalent circuit [11]. Figure 6 presents the connection between windings of induction machine and rotary transformer.

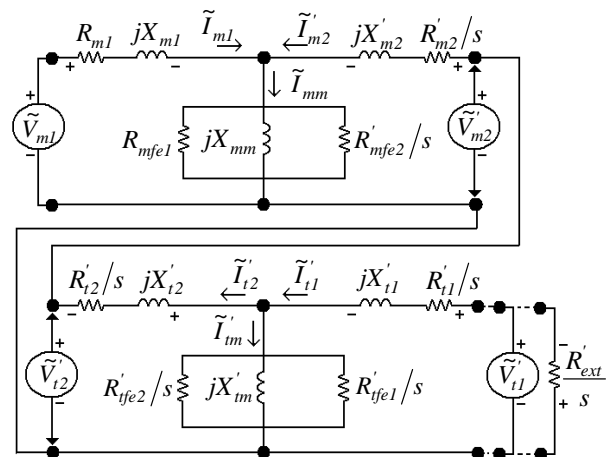


Figure 6 - Equivalent circuit of doubly fed induction machine with rotary transformer

From this model it is possible to analyze the machine operating at steady-state as motor and as



generator. All parameters are reflected to the stator of the induction machine.

5. PROTOTYPE DATA

Nominal data of the 90kW brushless doubly fed three-phase induction machine prototype are shown in table 2.

Table 2 - Nominal data of the prototype

V_{lm1}	I_{m1}	f_{m1}	$2 \cdot p_m$	P_{shaft}	V_{lm2}	S_t
690V	100A	60Hz	6	90kW	525V	90kVA

Figure 7 shows the prototype under test on laboratory facility.



Figure 7 - Doubly fed three-phase induction machine with rotary transformer on laboratory facilities

Figure 8 presents laboratory scheme for load tests on the doubly fed induction machine.

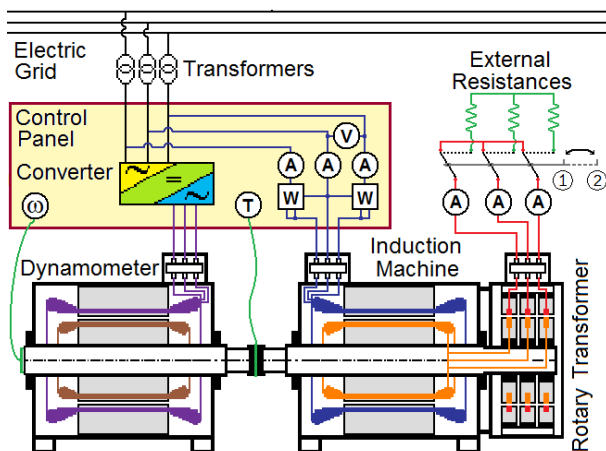


Figure 8 - Laboratory scheme for load tests

In Figure 8, it is possible to test doubly fed induction machine with transformer stator winding short-circuited or connected to resistances

switching between position 1 and 2, respectively. The instrumentation has the following meanings:

- A: amp meter
- V: voltmeter
- W: wattmeter
- ω : encoder
- T: torque transducer

Through open-circuit, short-circuit and no-load tests under the prototype presented on Figure 7, equivalent circuit parameters are obtained. Table 3 presents equivalent circuit parameters reflected to induction machine stator expressed in ohms (Ω).

Table 3 - Equivalent circuit parameters in ohms (Ω) @ 40°C

R_{m1}	X_{m1}	R_{m2}	X_{m2}	R_{mfe1}	X_{mn}	R_{mfe2}
0.036	0.284	0.038	0.291	454.8	9.69	1136
R_{t1}	X_{t1}	R_{t2}	X_{t2}	R_{tfe1}	X_{tm}	R_{tfe2}
0.019	0.131	0.017	0.139	102	3.24	102

6. STEADY-STATE MODEL RESULTS

By steady-state model and equivalent parameters circuit presented in table 3, it is possible to obtain performance curves of the prototype.

Figure 9 displays power curves of the doubly fed three-phase induction machine with rotary transformer. From 0 to 1 p.u. speed, the machine works as motor, transforming electrical power in mechanical power on shaft. From 1 to 2 p.u. speed, machine works as generator, converting mechanical power in electrical power injected on grid.

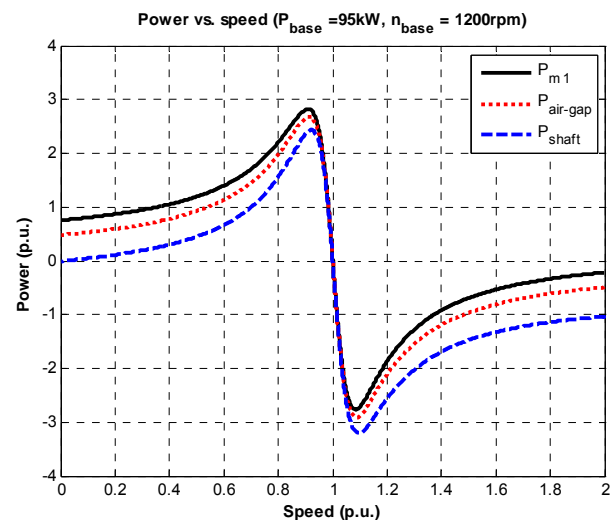


Figure 9 - Power for transformer stator winding short-circuited



Figure 10 shows the behavior of the diverse currents presented on the equivalent circuit from Figure 6.

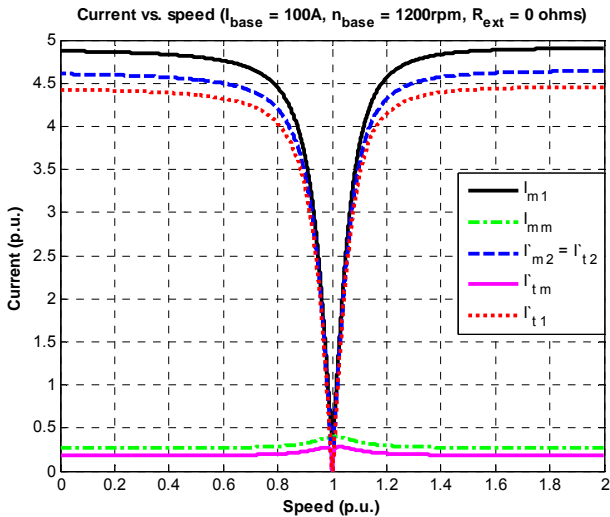


Figure 10 - Currents for short-circuited transformer stator winding

Like a conventional induction machine, the minimum current is verified at synchronous speed, when no active power is delivered on shaft. At synchronous speed, the current absorbed by induction machine stator is equal to its magnetizing current.

Figure 11 and 12 show that increasing external resistance to 0.23Ω and 0.41Ω (values referred to induction machine stator), it is possible to have higher starting torque and lower locked rotor current.

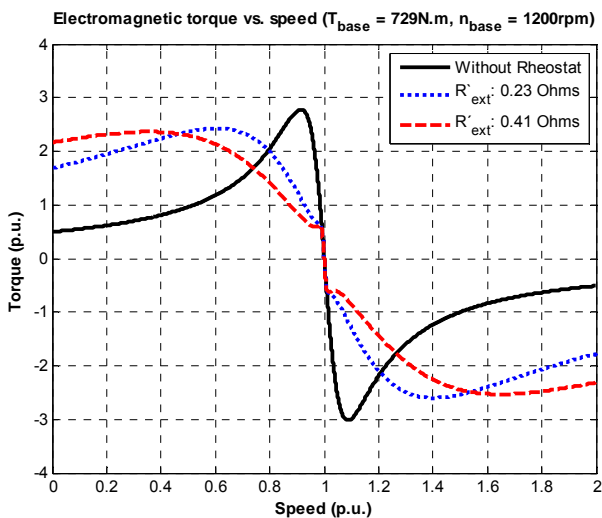


Figure 11 - Electromagnetic torques for transformer stator winding connected to external resistances

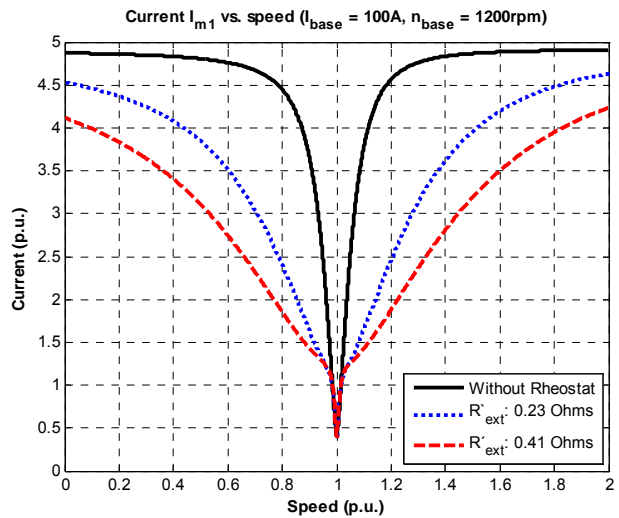


Figure 12 - Induction machine stator winding current for transformer stator winding connected to external resistances

The decreasing on maximum torque noticed in Figure 11 is consequence of low magnetizing reactance of this rotary transformer prototype. If increased its magnetizing reactance, the maximum torque decreasing should be smaller.

Tables IV and V present simulation results for 25% to 125% load for motor and generator regime. In both cases, rotary transformer stator winding is short-circuited.

Results for motor and generator regimes are close to each other. The main differences are related to speed, power absorbed or delivered to the grid and power factor.

Table 4 - Induction machine with rotor connected to rotary transformer (motor operation)

Simulation results					
Motor Operation					
Load	25%	50%	75%	100%	125%
V_{Im1} (V)	690	690	690	690	690
T_{shaft} (N.m)	183	367	548	729	907
P_{m1} (kW)	25.7	49.1	72.2	95.5	118
P_{shaft} (kW)	22.9	45.8	68.1	90.2	111
I_{m1} (A)	48.4	63.4	80.7	100	120
I_{t1} (A)	13.8	41.8	70.0	97.8	125
Efficiency (%)	89.4	93.3	94.3	94.5	94.3
Power factor	0.44	0.64	0.75	0.80	0.82
Speed (rpm)	1196	1191	1186	1181	1176



Table 5 - Induction machine with rotor connected to rotary transformer (generator operation)

Simulation results					
Generator Operation					
Load	25%	50%	75%	100%	125%
V_{im1} (V)	690	690	690	690	690
T_{shaft} (N.m)	183	367	548	729	907
P_{m1} (kW)	20.6	43.1	65.1	87.5	110
P_{shaft} (kW)	23.5	46.3	69.1	92.5	116
I_{m1} (A)	46.4	60.2	76.2	94.3	114
I_{tl} (A)	11.3	37.4	64.4	91.3	118
Efficiency (%)	88.6	93.1	94.3	94.6	94.5
Power factor	0.37	0.60	0.72	0.78	0.80
Speed (rpm)	1204	1208	1213	1217	1222

Stray losses of 0.5% of power from grid and mechanical losses of 1300W at 1200 rpm are considered in efficiency calculation.

7. LABORATORY MEASUREMENTS

Figure 13 shows the comparison between measured and simulated torque vs. speed curve for short-circuited transformer stator winding.

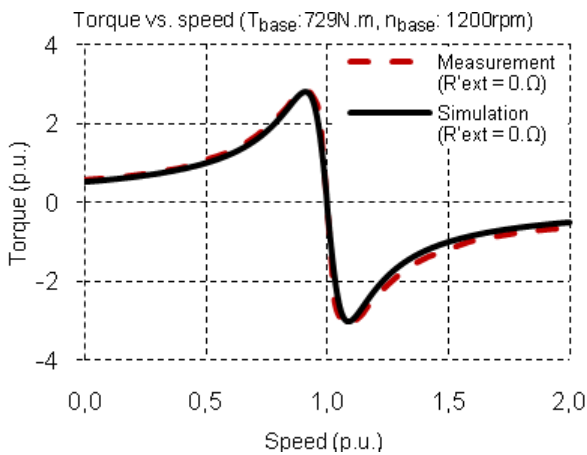


Figure 13 - Electromagnetic torque for transformer stator winding in short-circuit

Figure 14 shows measured and simulated current vs. speed curve for short-circuited transformer stator winding.

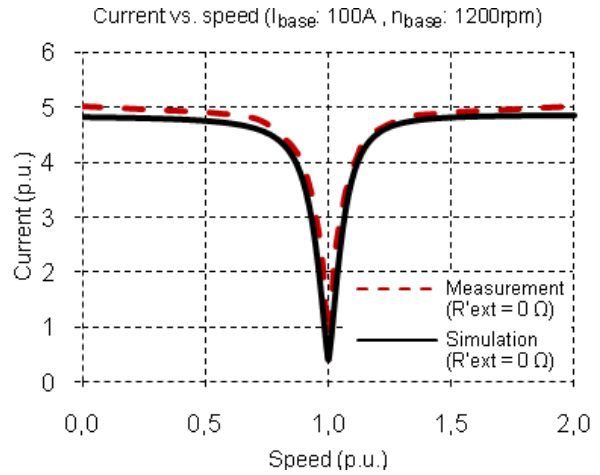


Figure 14 - Induction machine stator winding current for transformer stator winding in short-circuit

Figure 15 shows torque vs. speed curve considering the connection of an external resistance of 0.23Ω.

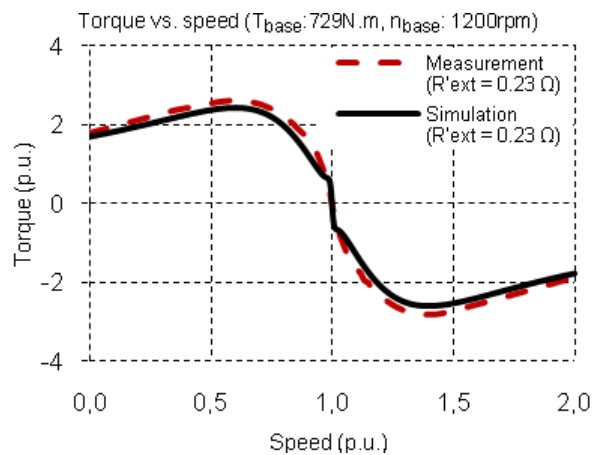


Figure 15 - Electromagnetic torques for transformer stator winding connected to external resistance of 0.23Ω (referred to induction machine stator)



In the same way, Figure 16 compares measured and simulated current vs. speed curve for the external resistance of 0.23Ω .

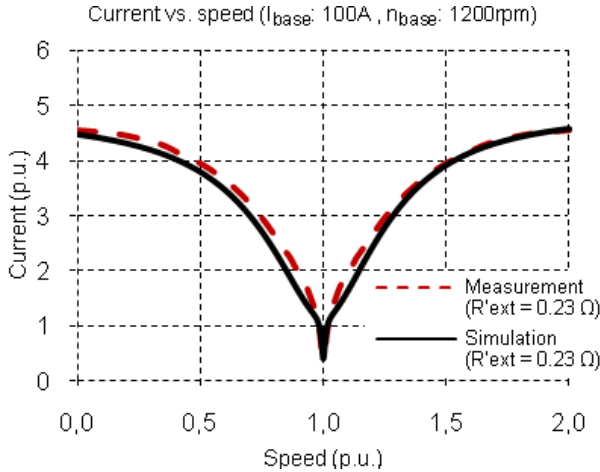


Figure 16 - Induction machine stator winding current for transformer stator winding connected to external resistance of 0.23Ω (referred to induction machine stator)

Figure 17 shows torque vs. speed curve when increasing external resistance to 0.41Ω .

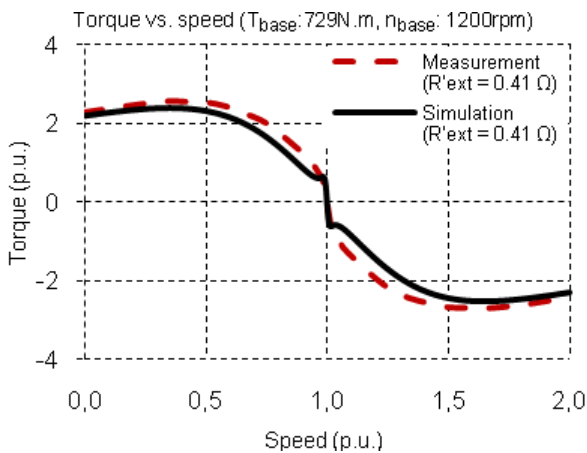


Figure 17 - Electromagnetic torques for transformer stator winding connected to external resistance of 0.41Ω (referred to induction machine stator)

Figure 18 compares measured and simulated current vs. speed curve for an external resistance of 0.41Ω .

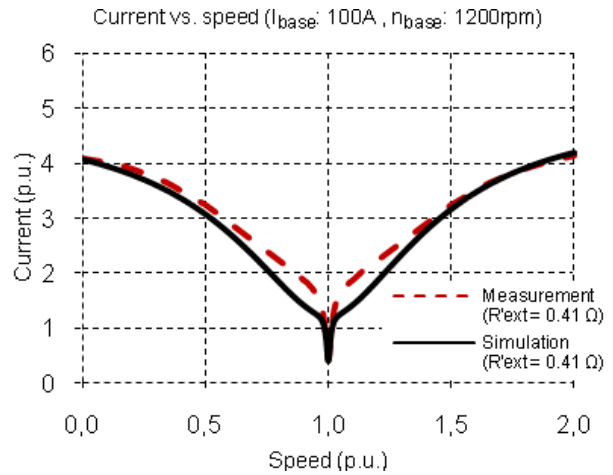


Figure 18 - Induction machine stator winding current for transformer stator winding connected to external resistance of 0.41Ω (referred to induction machine stator)

Figures. 13 - 18 show good agreement between measurement and simulation results, what confirms the assertively of the model. In Figure 18, the difference between measured and simulated current curves is consequence of some saturation on rotary transformer due to external resistance increasing. This effect is originated by adoption of linear values for rotary transformer parameters on steady state model.

Tables VI and VII present measurement results for 25% to 125% load for motor and generator regime. In both cases, rotary transformer stator winding is short-circuited.

Comparison between values presented on tables VI and VII with tables IV and V shows very good performance for steady state model in relation to measured values.

Power factor verified for this prototype is smaller than standard values for conventional 6 poles induction machines. Obviously, this reduction on power factor is explained by the inductive nature of rotary transformer [1].



Table 6 - Induction machine with rotor connected to rotary transformer (motor operation)

Measurement results					
Motor Operation					
Load	25%	50%	75%	100%	125%
V_{lm1} (V)	690	690	690	690	690
T_{shaft} (N.m)	182	364	546	728	910
P_{m1} (kW)	25.4	48.7	71.8	95.1	119
P_{shaft} (kW)	22.8	45.4	67.7	90.0	112
I_{m1} (A)	48.7	63.2	80.4	100	121
I_{tl} (A)	14.0	40.4	68.0	99.6	128
Efficiency (%)	89.8	93.5	94.4	94.6	94.2
Power factor	0.44	0.64	0.75	0.80	0.82
Speed (rpm)	1196	1191	1185	1181	1175

Table 7 - Induction machine with rotor connected to rotary transformer (generator operation)

Measurement results					
Generator Operation					
Load	25%	50%	75%	100%	125%
V_{lm1} (V)	690	690	690	690	690
T_{shaft} (N.m)	182	364	546	728	910
P_{m1} (kW)	20.4	42.8	65.6	88.0	110
P_{shaft} (kW)	23.0	46.1	69.4	92.8	116
I_{m1} (A)	46.1	60.0	77.2	96.2	116
I_{tl} (A)	13.0	37.4	64.6	94.9	121
Efficiency (%)	88.9	92.9	94.6	94.8	94.8
Power factor	0.37	0.60	0.71	0.77	0.80
Speed (rpm)	1205	1209	1214	1218	1223

8. CONCLUSION

Substituting brushes and slip-rings is the greatest advantage of using rotary transformers in doubly fed induction machines. Avoiding mechanical contact between brushes and slip-rings, motors and generators maintenance can be drastically reduced. Additionally, with the studied device, the installation of wound rotor machines on explosive environments becomes possible. Moreover, this solution keeps all the benefits inherent to the use of induction machine rotor circuit for machine controlling.

Results verified on prototype measurements are satisfactory and similar to steady-state model prediction. Performance verified in this machine gives good expectations about using doubly fed induction machine with rotary transformer as industrial motors and wind power generators.

9. ACKNOWLEDGMENT

Authors wish to thank WEG Equipamentos Elétricos S.A. for the prototype building and the use of its facilities.

10. REFERENCES

- [1] M. Ruviaro, F. Rincos, N. Sadowski, I. M. Borges, "Design and Analysis of a Brushless Induction Machine with Rotary Transformer", in XIX International Conference on Electrical Machines (ICEM), Rome, Italy, 2010.
- [2] F. Rincos, "Double-Fed in Cascade Brushless Three-Phase Asynchronous Machine" (in Portuguese), Master's dissertation, Universidade Federal de Santa Catarina, Brazil, 2001.
- [3] F. Rincos, N. Sadowski, R. Carlson, A. M. Oliveira, P. Kuo-Peng, "Performance Analysis of a Brushless Double Fed Cage Induction Generator", presented at Nordic Wind Power Conference, Chalmers University of Technology, Göteborg, Sweden, 2004.
- [4] F. Rincos, "Modeling, Project and Analysis of Brushless Double-Fed Three-Phase Asynchronous Machine" (in Portuguese), Doctoral thesis, Universidade Federal de Santa Catarina, Brazil, 2006.
- [5] N. Patin, E. Monmasson, J.-P. Louis, "Modeling and Control of a Cascaded Doubly Fed Induction Generator Dedicated to Isolated Grid", IEEE Transactions on Industrial Electronics, vol. 56, no. 10, pp. 4207-4219, Oct 2009.
- [6] S. Shao, E. Abdi, F. Barati, R. McMahan, "Stator-Flux-Oriented Vector Control for Brushless Doubly Fed Induction Generator", IEEE Transactions on Industrial Electronics, vol. 56, no. 10, pp. 4220-4228, Oct 2009.
- [7] F. Blazquez, C. Veganzones, D. Ramirez, C. Platero, "Characterization of the Rotor Magnetic Field in a Brushless Doubly-Fed Induction Machine", IEEE Transactions on Energy Conversion, vol 24, pp. 599 – 607, Sep 2009.
- [8] R. Datta, V.T. Ranganathan, "Variable-speed wind power generation using doubly fed wound rotor induction machine - a comparison with alternative schemes", IEEE Transactions on Energy Conversion, vol. 17, pp. 414, Sep 2002.
- [9] R.A. McMahan, P.C. Roberts, X. Wang, P.J. Tavner, "Performance of BDFM as generator and motor", IEE Proceedings Electric Power Applications, vol. 153, pp. 153, Mar 2006.
- [10] B. V. Gorti, G. C. Alexander, R. Spée, A. K. Wallace, "Characteristics of a Brushless Doubly-Fed Machine in Current-Fed Mode of Operation", in Proc. IEEE/IAS International Conference on Industrial Automation and Control, pp. 143-148, 1995.
- [11] P.C. Roberts, R.A. McMahan, P.J. Tavner, J.M. Maciejowski, T.J. Flack, "Equivalent Circuit for the brushless doubly fed machine (BDFM) including parameter estimation and experimental verification", IEE Proceedings Electric Power Applications, vol. 152, pp. 933, July 2005.
- [12] S. Williamson, A. C. Ferreira, A. K. Wallace, "Generalised Theory of the Doubly-Fed Machine. Part 1: Analysis", IEE Proceedings Electrical Power Application, vol. 144, n. 2, pp. 111-122, Mar 1997.
- [13] S. Williamson, A. C. Ferreira, "Generalised Theory of the Doubly-Fed Machine. Part 2: Model Verification and Performance", IEE Proceedings Electrical Power Application, vol. 144, n. 2, pp. 123-129, Mar 1997.
- [14] H. T. Ma, B. H. Chowdhury, "Working towards frequency regulation with wind plants: combined control approaches", IET Renewable Power Generation, Vol. 4, Iss. 4, pp. 308-316, 2010.
- [15] G. M. Joksimovic, "Double-fed Induction Machine-Dynamic Modeling using Winding Function Approach", in Proc. IEEE International Electric Machines and Drives Conference, pp. 694-697, 2007.



- [16] T. J. E. Miller, "Theory of the Doubly-Fed Induction Machine in the Steady State", in XIX International Conference on Electrical Machines (ICEM), Rome, Italy, 2010.
- [17] G. Ofner, O. Koenig, G. Dannerer, R. Seebacher, "Stedy State Modelling of Doubly Fed Induction Generators for Mega Watt Class Wind Turbines", in XIX International Conference on Electrical Machines (ICEM), Rome, Italy, 2010.
- [18] S. H. Marx, R. W. Rounds, "A Kilowatt Rotary Power Transformer", IEEE Transactions on Aerospace and Electronic Systems, vol. AES-7, issue 6, pp. 1157-1163, Nov. 1971.
- [19] J. Legranger, G. Friedrich, S. Vivier, J. C. Mipo, "Comparison of Two Optimal Rotary Transformer Designs for Highly Constrained Applications", in Proc IEEE Electric Machines & Drives Conference (IEMDC), pp. 1546-1515, 2007.
- [20] K.D. Papastergiou, D.E. Macpherson, "An Airborne Radar Power Supply With Contactless Transfer of Energy—Part I: Rotating Transformer", IEEE Transactions on Industrial Electronics, vol. 54, no. 5, pp. 2874-2884, Oct 2007.
- [21] K.D. Papastergiou, D.E. Macpherson, "An Airborne Radar Power Supply With Contactless Transfer of Energy—Part II: Converter Design", IEEE Transactions on Industrial Electronics, vol. 54, no. 5, pp. 2885-2893, Oct 2007.
- [22] K.D. Papastergiou, D.E. Macpherson, "Contact-less Transfer of Energy by means of a rotating transformer", in Proc. IEEE International Symposium on Industrial Electronics, pp. 1735-1740, 2005.
- [23] K.D. Papastergiou, D.E. Macpherson, "Air-gap effects in inductive energy transfer", IEEE Power Electronics Specialists Conference, pp. 4092-4097, 2008.
- [24] T.A. K. Stuart, H. R.J. Shamseddin, "Rotary Transformer Design with Fixed Magnetizing and/or Leakage Inductances", IEEE Transactions on Aerospace and Electronic Systems, AES-22, pp. 565, Sep 1986.
- [25] J.P.C. Smeets, L. Encica, E.A. Lomonova, "Comparison of winding topologies in a pot core rotating transformer", presented at 12th International Conference on Optimization of Electrical and Electronic Equipment (OPTIM), Brasov, Romania, 2010.
- [26] Yu-Ting Huang, Chi-Jen Chen, Wen-Ben Shu, "Finite Element Analysis on Characteristics of Rotary Transformer", IEEE Transactions on Magnetics, vol. 30, pp. 4866, Nov 1994.
- [27] R. Mecke, "Contactless Inductive Energy Transmission Systems with Large Air Gap", in Proc. European Conference on Power Electronics and Applications, 2001.
- [28] J. Legranger, G. Friedrich, S. Vivier, J. C. Mipo, "Design of a Brushless Rotor Supply for a Wound Rotor Synchronous Machine for Integrated Starter Generator", in Proc IEEE Vehicle Power and Propulsion Conference, pp. 236-241, 2007.
- [29] C. Wm. T. McLyman, "Transformer and Inductor Design Handbook", 3rd ed., Chapter 19, Ed. New York: Marcel Dekker Inc., 2004.

11. BIOGRAPHIES

Maurício Ruviano is Electrical Engineer at WEG Equipamentos Elétricos S.A. and Master's student at Universidade Federal de Santa Catarina. He received his Engineering Diploma from the same university in 2006. His work and research topics are electrical calculation of large induction machines and wind energy generation.

Fredemar Runcos is Engineering Manager at WEG Equipamentos Elétricos S.A. and Professor at Centro Universitário de Jaraguá do Sul – PUC-UNERJ. He received his Doctoral Diploma from Universidade Federal de Santa Catarina at 2006. His work and research topics are induction and synchronous machines. He is author or co-author of nearly 20 technical papers in journals and conferences.

Nelson Sadowski is full Professor at the Universidade Federal de Santa Catarina. He received his Doctoral Diploma from de Institut National Polytechnique de Toulouse at 1993 and his Habilitation à la Direction des Recherches from the same institute at 2002. His research topics are the calculation of electromagnetic fields by numerical methods. He is author or co-author of nearly 300 technical papers in journals as well as in conferences. With Professor Joao Pedro Assumpção Bastos, he is author of the book Electromagnetic Modeling by Finite Elements Methods.

Iduan Machado Borges is Mechanical Engineer at WEG Equipamentos Elétricos S.A. He received his Engineering Diploma from Universidade Federal de Santa Catarina at 2008. His work topics are the structural calculation of large induction machines.